CHINESE JOURNAL OF MECHANICAL ENGINEERING
Vol. 28, No. 4, 2015

DOI: 10.3901/CJME.2015.0414.042, available online at www.springerlink.com; www.cjmenet.com; www.cjme.com.cn

Stiffness Analysis of Corrugated Flexure Beam Used in Compliant Mechanisms

WANG Nianfeng*, LIANG Xiaohe, and ZHANG Xianmin

Guangdong Province Key Laboratory of Precision Equipment and Manufacturing Technology, South China University of Technology, Guangzhou 510641, China

Received June 23, 2014; revised March 31, 2015; accepted April 14, 2015

Abstract: Conventional flexible joints generally have limited range of motion and high stress concentration. To overcome these shortcomings, corrugated flexure beam(CF beam) is designed because of its large flexibility obtained from longer overall length on the same span. The successful design of compliant mechanisms using CF beam requires manipulation of the stiffnesses as the design variables. Empirical equations of the CF beam stiffness components, except of the torsional stiffness, are obtained by curve-fitting method. The application ranges of all the parameters in each empirical equation are also discussed. The ratio of off-axis to axial stiffness is considered as a key characteristic of an effective compliant joint. And parameter study shows that the radius of semi-circular segment and the length of straight segment contribute most to the ratio. At last, CF beam is used to design translational and rotational flexible joints, which also verifies the validity of the empirical equations. CF beam with large flexibility is presented, and empirical equations of its stiffness are proposed to facilitate the design of flexible joint with large range of motion.

Keywords: corrugated flexure beam, stiffness analysis, compliant mechanisms

1 Introduction

Unlike rigid-link mechanisms, a compliant mechanism is a mechanism that gains some or all of its mobility from elastic deformation of its flexible components instead of rigid links and movable joints[1–2]. It is designed to accomplish with a one-piece device what conventional mechanisms can do with multiple pieces. The applications of compliant mechanisms are unlimited, both in the macro domain and micro domain, for instance, for high precision manipulation stages[3–4], instruments for minimally invasive surgery[5–7], and Micro-Electromechanical Systems/Nano-Electromechanical Systems(MEMS/NEMS)[8–10]. These systems generally require a reduced system weight, high precision, and simple control schemes that compliant mechanisms can offer.

Elastic deformation of flexible components complicates the analysis of compliant mechanisms. Along with the development of compliant mechanisms, there has been a growing interest in the area of systematic approaches in compliant mechanism synthesis. Two main approaches have been developed for systematic synthesis of compliant mechanisms, a Pseudo-Rigid-Body(PRB) approach[11] and a topology optimization approach[12–19]. PRB approach, which connects compliant mechanism directly to rigid-body mechanism theory, is a major approach to analyze the statics and kinematics of flexible components. The flexible joints design is the crucial part of design based on PRB method. In the last 60 years, many flexible joints have been researched and developed for compliant mechanisms design[2, 20–22]. Most of the flexure joints are assembled from notch joints[23] or/and leaf spring joints[24–27] by reason that they are well understood by many researchers and designers and they can basically meet the design requirements. Ideally, a flexible joint must contain the qualities of large range of motion, minimal axis drift, increased off-axis stiffness, reduced stress concentrations and ease of manufacture. To the best of our knowledge, none of the existing flexible joints has all the qualities. Notch joints and leaf spring joints have simple structure and acceptable off-axis stiffness but limited motion, and notch joints have stress concentration.

With the same cross section, the stiffness of flexure beam is only related to its overall length[28], which means that the longer the overall length the smaller the stiffness. If the spans are same in the longitudinal direction, a corrugated beam will have a longer centerline which will increase the actual length of beam to deform. Based on above observations, our previous paper[29] introduces a new type of flexure structure, corrugated flexure(CF) beam, and proposes a pseudo-rigid-body model for it. As the successful design of compliant mechanisms using CF beam requires knowledge of the kinematics and manipulation of

* Corresponding author. E-mail: menfwang@scut.edu.cn
Supported by National Natural Science Foundation of China(Grant Nos. 51205134, 91223201), Doctoral Fund of Ministry of Education of China(Grant No. 20120172120001), and Research Project of State Key Laboratory of Mechanical System and Vibration, China(Grant No. MSV201405).

the stiffnesses as the design variables, the empirical equations of stiffness of CF beam are established and their application ranges are discussed. Section 2 outlines the corrugated flexure beam. The solution for stiffness of CF beam is described in section 3. Parameter study is carried out in section 4. A translational joint and a rotational joint based on CF beam are designed in section 5. Some concluding remarks are given in section 6.

2 Corrugated Flexure Beam

CF beam is a periodical corrugated structure where each repeated unit(blue part shown in Fig. 1) consists of a semi-circular and two straight segments. The CF beam shown in the figure is composed of 8 units. The cross section of CF beam is rectangle. Actually it can be circle, ellipse or other shapes. The parameters of the CF beam are as follows: the number of units N(N is even), width w and thickness t of cross section, length $l/2$ of straight segment, radius R of semi-circular segment, and the span length L.

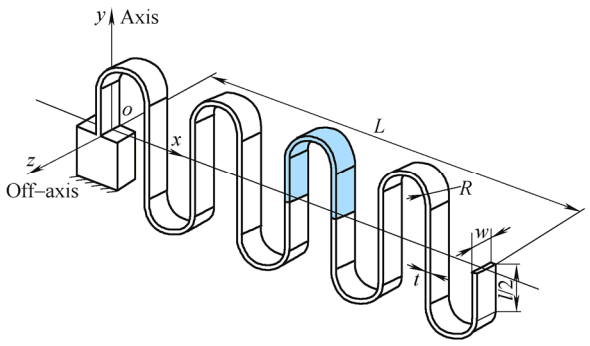

Fig. 1. Corrugated flexure beam

One of the parameters that should be studied to make sure a CF beam is able to execute a task accurately is stiffness of the CF beam. The complete form of the stiffness of the CF beam is formulated parametrically and discussed in next two sections.

3 Stiffness Equations of CF Beam

Each stiffness component has a definite effect on the character of CF beam, but there is no simple yet rigorous method to calculate these stiffness values. Screw theory[30–32] is a common approach to solve the stiffness derivation of some flexible joints and mechanism with small deformation. Through searching the literature, axial stiffness(translational stiffness of y-axis)[33] and rotational stiffness of z-axis[2, 34] has been mentioned, but other stiffness components are being looked at. All the empirical equations of the CF beam stiffness are obtained by curve-fitting. Because of similarity, only the equation of axial stiffness is discussed in detail. Initially the parameters of CF beam are studied through Finite Element Analysis(FEA). Then, an approximate form of the empirical equation is given. Lastly, the relationship between each two parameters is found out and the final empirical equation is determined.

3.1 Axial stiffness

The material used for CF beams is 60Si2Mn. The Young's modulus E assumed is 206 GPa with Poisson's ratio of 0.29 and yield strength of 1176 MPa. The data used for curve fitting are acquired through the control variate method using Workbench.

Through FEA of CF beam, it can be concluded that N, R and l have an inverse relationship with axial stiffness, but w, t and the elastic modulus E are positively related to it. Thus the empirical formula can be assumed to be a fraction. E, w and t are in the numerator, and N, R and l are in the denominator. Corresponding to increasing R, measured data are well fitted by a linear line, which can be expressed as follows:

$$\begin{aligned}
&R=1: K_y^{-1}=2.359\ 8l+6.594\ 1,\\
&R=2: K_y^{-1}=9.386\ 8l+54.799\ 3,\\
&R=3: K_y^{-1}=21.131\ 8l+186.796\ 4,\\
&R=4: K_y^{-1}=38.659\ 6l+464.173\ 3,\\
&R=5: K_y^{-1}=59.900\ 8l+894.765\ 6,\\
&R=6: K_y^{-1}=85.91l+1\ 539.142\ 2,\\
&R=7: K_y^{-1}=116.594\ 3l+2\ 443.058\ 7,
\end{aligned} \tag{1}$$

when N=16, w=5 mm, t=0.3 mm. K_y is the axial stiffness of CF beam.

Next are two regression functions k_1 and k_2 fitted to the coefficients and constants of the above fitted equations respectively. They can be expressed as follows:

$$\begin{aligned}
k_1 &= 2.384\ 3R^2+0.018\ 9,\\
k_2 &= 7.127\ 6R^3+0.187.
\end{aligned} \tag{2}$$

Then $1/K_y = k_1 l + k_2$ can be approximately expressed as

$$K_y^{-1}=2.384\ 3R^2l+7.127\ 6R^3. \tag{3}$$

Fitted equations about other parameters other than R can be obtained similarly. Take E into account, carry out some transformation, and then axial stiffness can be written as

$$K_y=\frac{10^{-2}E(6.5wt^3-0.82t^3+0.000\ 512)}{N^3R^2(l+3R)}. \tag{4}$$

Many parametric studies were performed on the stiffness equation of the CF beam to create a catalog of graphs that serves as a quick look at the characteristics of the CF beam.

The parametric studies are represented by 3-D surface plots of the output variables. The relationship between K_y

and each parameter except N is visualized in Fig. 2. Fig. 2(a) shows the combined effects of length and radius on K_y for given width and thickness. To maximize the desired stiffness, R and l must be minimized. Fig. 2(b) shows the combined effects of width and thickness on K_y for given length and radius. Beam width has a linear effect on stiffness for a given beam thickness. However, beam thickness nonlinearly increases the stiffness for a given width.

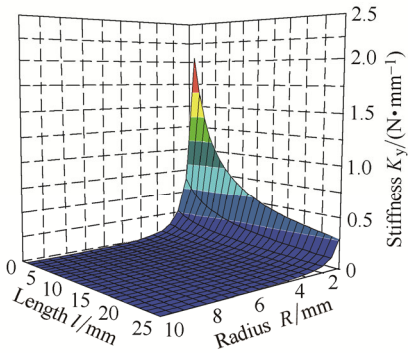

(a) N=12, w=5 mm, t=0.6 mm

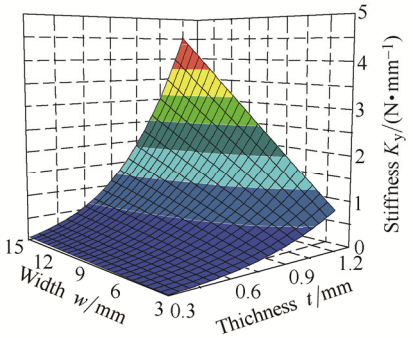

(b) N=12, R=2 mm, l=5 mm

Fig. 2. 3-D surface plots of axial stiffness K_y

K_y found by Eq. (4) will be compared with numerical method in order to estimate its accuracy. Various types of CF beams shown in Fig. 3 were used. The analytical values obtained from equation and simulation values obtained from FEA are tabulated in Table 1, where "N30-R10-l150-t2-w30" means that N=30, R=10 mm, l=150 mm, t=2 mm and w=30 mm. The results in Table 1 show that the largest error is 5.15% which is within acceptable limit.

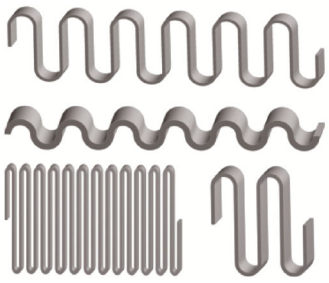

Fig. 3. Various types of CF beams

Table 1. Analytical and simulation values of K_y (N/mm)

Parameter	Analytical value	Simulation value	Error
N30-R10-l150-t2-w30	0.006 58	0.006 40	2.82%
N16-R3.5-l5-t0.3-w10	0.004 62	0.004 59	0.33%
N12-R2-l20-t1-w7	0.512 20	0.485 80	5.15%
N12-R8-l10-t1-w15	0.052 97	0.051 82	2.15%

The data used in curve fitting of K_y are collected when parameters are in the ranges: N=6–16, R=1–7 mm, l=0–16 mm, w=2–10 mm, and t=0.1–0.4 mm. The results in Table 1 show that Eq. (4) can also apply to the case where parameters are out of their ranges defined in data collection. Further research indicates that it should be avoided that R and l get close to their lower limits simultaneously, because the error increases rapidly in that case.

3.2 *x*-axis translational stiffness

By the same way used above, x-axis translational stiffness can be determined as

$$K_x = \frac{Ewt^3}{Nk_{x1}}, \tag{5}$$

where k_{x1} is given by

$$k_{x1} = l^3 + (9.34R - 1.52)l^2 + (-2.1R^3 + 44.1R^2 - 57.33R + 41.12)l + (16R^3 + 9.11R^2 - 17.4R + 7.84). \tag{6}$$

As Eq. (5) shown, there is a cubic relationship between stiffness and beam thickness, and width has only a linear effect on stiffness. There is a very complex relationship between R, l and stiffness K_x. The application ranges of K_x are: $N \geqslant 2$, $t \geqslant 0.1$ mm, $w \geqslant 2$ mm, and R and l can be any positive rational numbers.

Axis drift can be counteracted by the symmetry of the configuration, but CF beam is not symmetric about the x-axis, and there will be a large axis drift when loaded in the negative direction of x-axis. Because of the asymmetry, accuracy of the equation K_x decreases heavily as the deformation becomes larger. An acceptable K_x-value can be obtained through Eq. (5) only if the deformation is small. Moreover, it generates a small axis drift when CF beam is loaded in the positive direction of x-axis, and in this case CF beam can be interpreted as extension spring.

The relationship between K_x and each parameter except N is visualized as shown in Fig. 4. Fig. 4(a) shows the combined effects of length and radius on K_x for given width and thickness, while Fig. 4(b) shows the combined effects of width and thickness on K_x for given length and radius.

3.3 Off-axis stiffness

Off-axis stiffness can be expressed as

$$K_z = \frac{10^{-2} Et^3 (0.26w^2 + 8.064w)}{N^3 (lR^2 + 1.5R^3 + 0.3R^2 - 3.7R + 2)}. \tag{7}$$

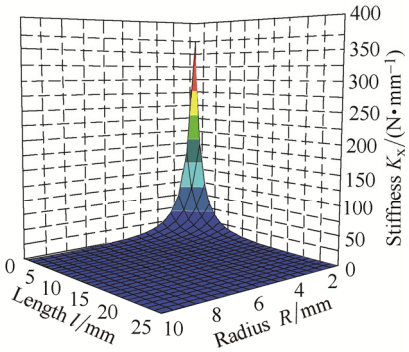

(a) N=12, w=5 mm, t=0.6 mm

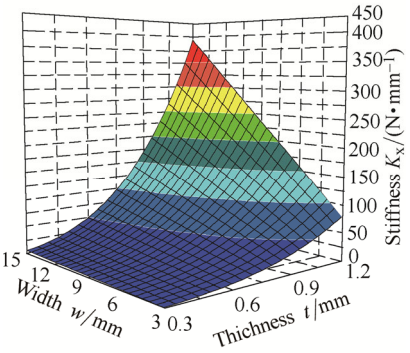

(b) N=12, w=2 mm, l=5 mm

Fig. 4. 3-D surface plots of x-axis translational stiffness

The application ranges of K_z are $N \geqslant 2$, $R \geqslant 1$ mm, $l \geqslant 2$ mm, 1.5 mm$\geqslant t \geqslant$0.1 mm, and $w \geqslant 2$ mm. It is worth noting that: error increases as N decreases; error increases rapidly as R and l get close to their lower limits simultaneously; and width should be much larger than thickness. Moreover, this equation can only be applied to the case where the CF beam is at small deformation.

The relationship between K_z and each parameter except N is visualized as shown in Fig. 5. Fig. 5(a) shows the combined effects of length and radius on K_z for given width and thickness, while Fig. 5(b) shows the combined effects of width and thickness on K_z for given length and radius.

3.4 *y*-axis rotational stiffness

In solving rotational stiffnesses, the ranges of parameter in data collection are as follows: R=1–5 mm, l=2–14 mm, w=3–7 mm, t=0.2–0.4 mm, and N=4–16.

By the same way as that used to solve K_y, y-axis rotational stiffness can be formulated as

$$K_{ry} = \frac{E((0.15w-0.293)t^3 + 0.155t^2 - 0.037\ 5t + 0.002\ 85)}{N(l + 1.76R - 1.58)}. \tag{8}$$

The application ranges of K_{ry} are: $N \geqslant 4$, $R \geqslant 1$ mm, $l \geqslant 1$ mm, 1.5 mm$\geqslant t \geqslant$0.2 mm, and 15 mm$\geqslant w \geqslant$2 mm. It is worth noting that error increases significantly as R and l get close to their lower limit simultaneously. The ratio of w/t had better decrease as t increases; for instance, the w/t ratio should less than 15 when t=1 mm, while the w/t ratio should less than 10 when t=1.5 mm.

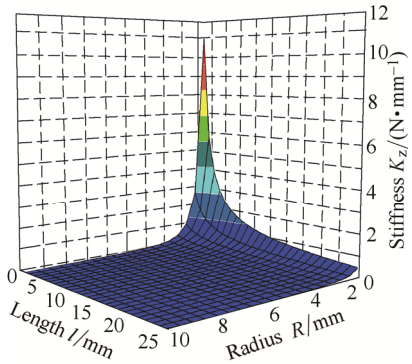

(a) N=12, w=5 mm, t=0.6 mm

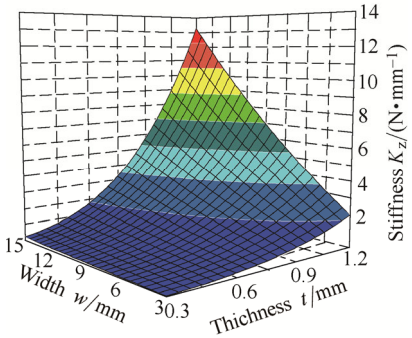

(b) N=12, R=2 mm, l=5 mm

Fig. 5. 3-D surface plots of off-axis stiffness

The relationship between K_{ry} and each parameter except N is visualized as shown in Fig. 6. Fig. 6(a) shows the combined effects of length and radius on K_{ry} for given w and t, while Fig. 6(b) shows the combined effects of width and thickness on K_{ry} for given length and radius.

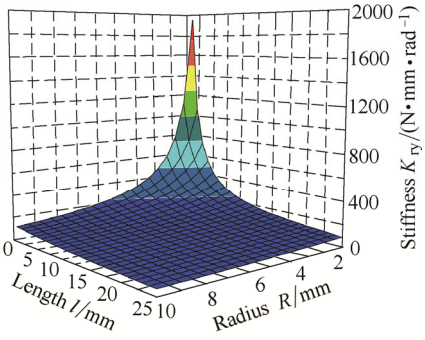

(a) N=12, w=5 mm, t=0.6 mm

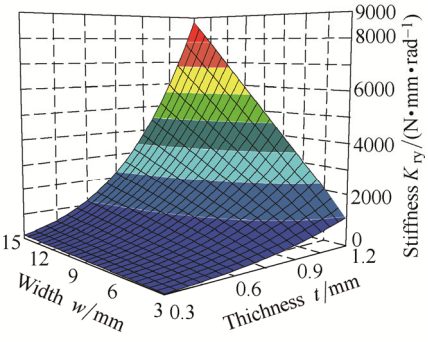

(b) N=12, R=2 mm, l=5 mm

Fig. 6. 3-D surface plots of y-axis rotational stiffness

3.5 *z*-axis rotational stiffness

According to Euler-Bernoulli beam theory, the deflection angle of a simple cantilever beam can be described using the following formula: $\theta=\boldsymbol{M}L_0/EI$. Here, θ is deflection angle at the free end of a cantilever beam shown in Fig. 7, and L_0 is the total length of a cantilever beam. When a pure moment loading is applied to a fixed-pinned CF beam at the free end, M is constant along the beam centerline. If it is assumed that the CF beam behaves elastically for the moment loading, the resulting final rotation of the loaded beam is simply the sum of the rotations of all units. Therefore, the motion of the system may be interpreted as the superposition of the motion of N single units.

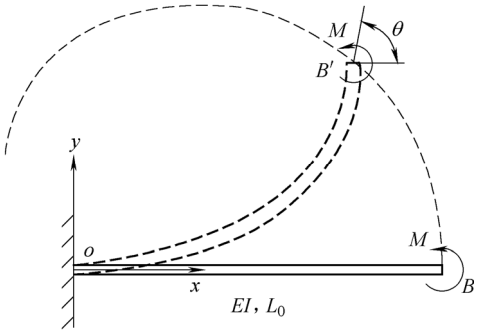

Fig. 7. Straight cantilever beam behaves elastically for the moment loading

As a result, the expression of K_{rz} can be written as

$$K_{rz}=\frac{1.06EI}{N(l+\pi R)}, \tag{9}$$

where $N(l+\pi R)$ means the total length of CF beam, coefficient 1.06 is determined from the measured data, and I is the moment of inertia.

The relationship between K_{rz} and each parameter except N is visualized as shown in Fig. 8. Fig. 8(a) shows the combined effects of length and radius on K_{rz} for given width and thickness, while Fig. 8(b) shows the combined effects of width and thickness on K_{rz} for given length and radius.

The above two expressions, K_{ry} and K_{rz}, can be applied to large-deformation CF beam.

3.6 Torsional stiffness

Quantitative expression of torsional stiffness K_{rx} cannot be given because the equation changes once the parameter values are out of the range in which the data used in curve fitting were generated. The expression of torsional stiffness of straight cantilever beam can be obtained through introducing correction factor which depends on the w/t ratio[35]. But the correction factor method is invalid for CF beam. Therefore, only slices of a 3-D volume are used to indicate K_{rx} instead of equation. Fig. 9(a) shows the tendency of K_{rx} as N, w and t change when L is 16 mm. K_{rx} increases with respect to N, w and t. L is constant and $L=2RN$, so R changes accordingly when N changed, which means that R has an inverse relationship with K_{rx} for a given L. Measured data indicate that l has little effect on K_{rx}, so it is unnecessary to take l into account. For easy illustration, the denary logarithm of K_{rx} is plotted in Fig. 9. Fig. 9(b) shows the tendency of K_{rx} as N, w and t change when R is 1.5 mm. It is evident that increased width, thickness and reduced N are required to increase K_{rx} for a given R.

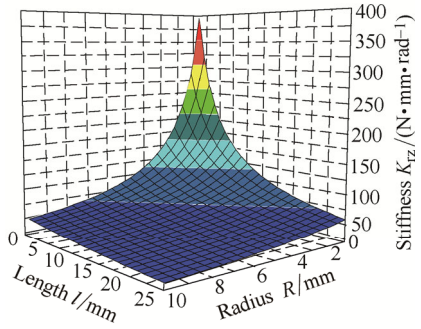

(a) N=12, w=5 mm, t=0.6 mm

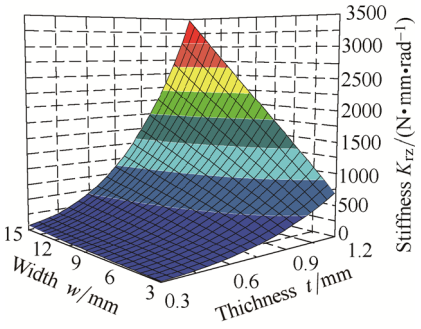

(b) N=12, R=2 mm, l=5 mm

Fig. 8. 3-D surface plots of *z*-axis rotational stiffness

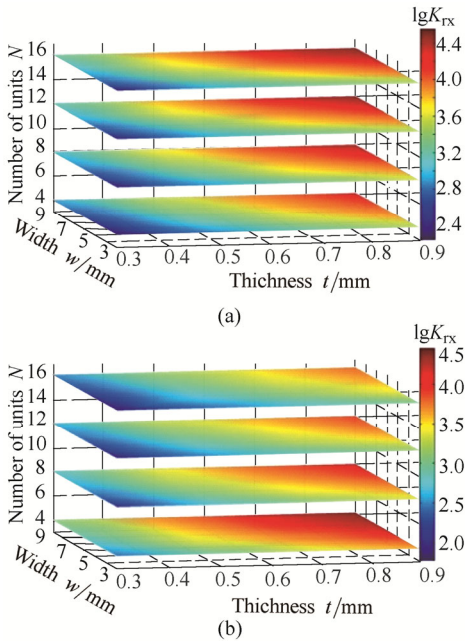

Fig. 9. Slices of a 3-D volume used to indicate K_{rx}

4 Parameter Study

Compliant joints deliver a high degree of compliance in

the desired direction, but suffer from low rotational and translational stiffness in other directions. The ratio of off-axis to axial stiffness is considered as a key characteristic of an effective compliant joint. CF beam will be used to design compliant joints in next section, so parameter study should be carried out.

The stiffnesses of a typically sized CF beam and a straight cantilever beam are calculated and the results are shown in Table 2. The ratio of each stiffness with respect to K_y is also included. K_{sy} is the axial stiffness of a straight cantilever beam. The results in Table 2 show that K_x is much larger than others, and K_z is larger than K_y. Therefore, if used as a translational joint, the desired motion direction should be y-axis direction, and K_x/K_y and K_z/K_y should increase so as to increase the ratio of off-axis to axial stiffness. In a similar way, if used as a rotational joint, z-axis should be center of rotation.

Table 2. Stiffness-values
(N=16, R=2 mm, l=12 mm, w=5 mm, t=0.5 mm)

Stiffness	Value from formulas	Ratio to K_y
Axial stiffness K_y / (N • mm^{-1})	0.027 7	1
Stiffness of straight beam K_{sy}/ (N • mm^{-1})	0.120	4.33
Translational stiffness K_x / (N • mm^{-1})	1.50	54.1
Off-axis stiffness K_z / (N • mm^{-1})	0.052 7	1.90
Torsional stiffness K_{rx} / (N • mm • rad^{-1})	377	13 600 mm^2 • rad^{-1}
Rotational stiffness K_{ry} / (N • mm • rad^{-1})	73.8	2660 mm^2 • rad^{-1}
Rotational stiffness K_{rz} / (N • mm • rad^{-1})	38.9	1400 mm^2 • rad^{-1}

As Fig. 10 shown, l-value has a great effect on K_x/K_y. K_x/K_y is almost entirely unaffected by w and t, which can be predicted by Eqs. (4) and (5). K_x/K_y is generally very large, so only K_z/K_y is taken into account. From Eqs. (4) and (7), it is obviously that N has no effect on K_z/K_y, and effect caused by t is small. Thus, N and t can be flexibly configured during designing.

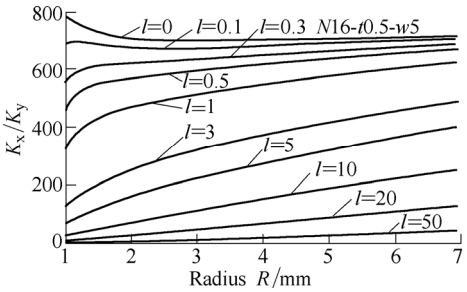

Fig. 10. Relationship between K_x/K_y and l, R.

Fig. 11(a) shows that K_z/K_y decreases as R increases when l is less than a certain value(approximately 4 mm), but increases with respect to R when l is greater than that value. And K_z/K_y has an inverse relationship with l. To maximize the ratio of off-axis to axial stiffness, l should be minimized. In fact, when R=0 and l=0, CF beam will turn into straight beam, and K_z/K_y becomes maximal. Fig. 11(b) shows that K_z/K_y increases slowly as w increases, that is to say, K_z/K_y has a low sensitivity to w.

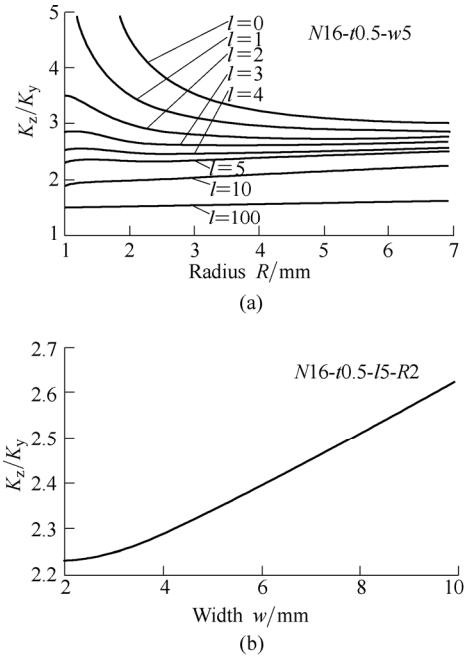

Fig. 11. Relationship between K_z/K_y and l, R, w

Without equation of K_{rx}, its value can be only obtained by means of FEA or experiment. As l has little effect on K_{rx}, it can be made full use to work out an acceptable K_{rx}/K_{rz}. The results of FEA show that K_{rx}/K_{rz} is much larger than 1. Therefore, an acceptable K_{ry}/K_{rz} can be worked out preferentially and then the K_{rx}/K_{rz} will be verified.

The R-K_{ry}/K_{rz} curves in Fig. 12(a) are similar to those in Fig. 11(a). Reduced R and l are required to increase K_{ry}/K_{rz}. In Fig. 12(b), K_{ry}/K_{rz} reaches a peak when t is approximately equal to 0.3 mm. Therefore, t for peak and larger w can increase K_{ry}/K_{rz}.

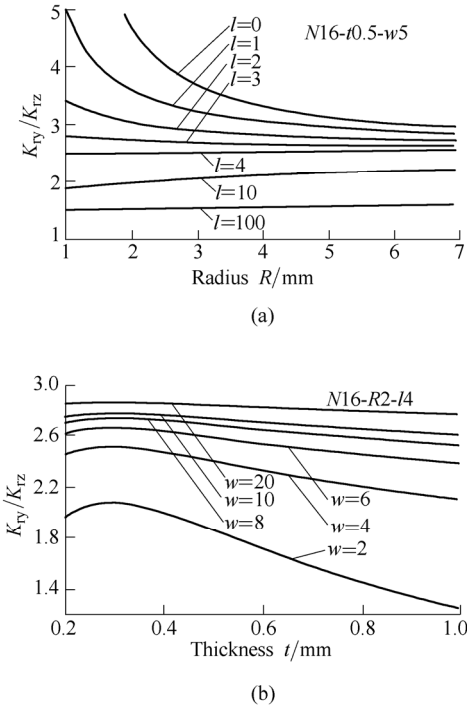

Fig. 12. Relationship between K_{ry}/K_{rz} and l, R, t, w

Table 3 indicates that K_z/K_y increases after parameters are adjusted, but K_{sy}/K_y decreases at the same time. The larger the K_z/K_y is, the smaller the K_{sy}/K_y. A large K_z/K_y value indicates a high ratio of off-axis to axial stiffness, while a large K_{sy}/K_y-value indicates a large flexibility. There is a balance between them. R and l are key parameters to be preferentially considered during designing.

Table 3. Stiffness-values
(N=16, R=1 mm, l=0, w=7 mm, t=0.4 mm)

Stiffness	Value from formulas	Ratio to K_y
Axial stiffness K_y / (N • mm^{-1})	0.479	1
Stiffness of straight beam K_{sy}/ (N • mm^{-1})	0.678	1.42
Translational stiffness K_x / (N • mm^{-1})	371	774
Off-axis stiffness K_z / (N • mm^{-1})	22.3	46.5
Torsional stiffness K_{rx} / (N • mm • rad^{-1})	580	1210 mm^2 • rad^{-1}
Rotational stiffness K_{ry} / (N • mm • rad^{-1})	4370	9120 mm^2 • rad^{-1}
Rotational stiffness K_{rz} / (N • mm • rad^{-1})	162	338 mm^2 • rad^{-1}

5 Design Example

Like some other flexible segments, CF beam can be applied to design translational and revolute joints. In this section, two examples are presented to demonstrate the benefits of CF beam and verify the empirical equations.

5.1 Corrugated flexure translational joint

Fig. 13(a) shows a kind of compliant translational(CT) joint composed of leaf springs. High stiffness limits its range of motion. In order to decrease the stiffness, CF beams take the place of leaf springs as shown in Fig. 13(b). This new joint is called the Corrugated Flexure Translational(CFT) joint.

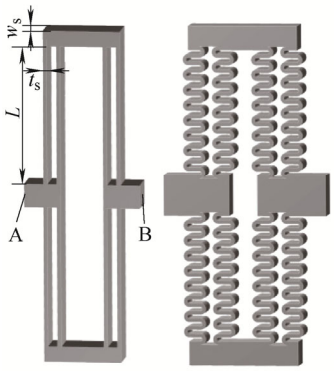

Fig. 13. CF joint and CFT joint

The parameters used are as follows: w_s=10 mm, t_s=1 mm and L=36 mm. The material is spring steel 60Si2Mn. Face A is fixed and face B is the free end. The translational stiffness of single leaf spring K_s can be obtained in the realm of linear theory using the equation $K_s=Ewt^3/L^3$. Use CF beams to replace leaf springs, make sure that K_s is 3 times as K_y, and meanwhile, K_z/K_y and K_x/K_y should be designed as large as possible. It is known that $w=w_s$, $t = t_s$ and L are constant. The next step is to determine N, R and l.

According to the results presented in the previous section, N can be any even number because it has little effect on K_z/K_y. The initial N and R are given as N=12, R=1.5 mm. Then l=4.74 mm and K_z/K_y=2.688 according to Eqs. (4) and (7). When N=18 and R=1 mm, it can obtain that l=3.16 mm and K_z/K_y=3.14. When R decreases, relative error of translational stiffness increases. Therefore, the parameters of CFT joint are finally decided as R=1 mm, l=3.16 mm, w=10 mm, t=1 mm, and N=18.

The total stiffness of CFT joint is $8K_y$. When the applied force equals to 10 N, the displacement of CFT joint is 0.353 mm while displacement of CT joint is 0.11 mm. Fig. 14 displays structural deformation graph. The results indicate that CFT joint offers the benefits of large range of motion.

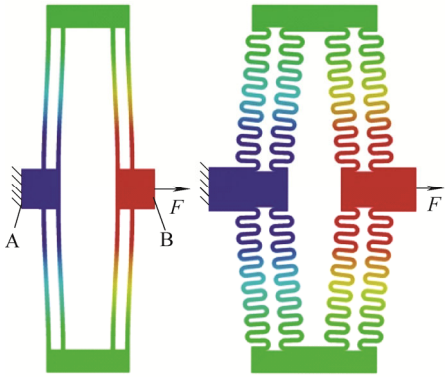

Fig. 14. CF joint and CFT joint with force loading

5.2 Corrugated flexure revolute joint

Flexible revolute joints are designed to generate pure rotational motion. Small-length flexural pivot(see Fig. 15(a)) is a simple and flexible revolute joint. Starting from small-length flexural pivot, a new kind of revolute joint, Corrugated Flexible Revolute(CFR) joint(see Fig. 15(b)), is designed.

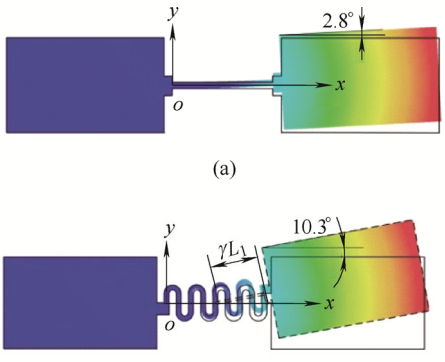

Fig. 15. Small-length flexural pivot and CFR joint

The design process of CFR joint is similar to that of CFT joint. After K_{rz}, w and t are given, the first step is to decide N and R based on the results in section 5. And then l and K_{ry}/K_{rz} are calculated using Eqs. (8) and (9). Repeat the above steps, and finally determine the acceptable

parameters. In Fig. 15, flexible segments of small-length flexural pivot and CFR joint have the same span, width and thickness. Parameters of the flexible segment of CFR joint are: R=1 mm, l=3 mm, w=5 mm, t=0.8 mm, and N=8. With the same moment loading, their rotation angles are shown in Fig. 15.

Rotational stiffness and load decide the deformation angle while rotational center decides the position of free end. The position of rotational center of CFR joint will be decided through Eq. (9) and FEA. The characteristic radius factor γ is equal to l_1/L_1, where L_1=2RN and l_1 is the characteristic radius.

Fig. 16 shows the γ-values for ten kinds of CFR joints whose parameters are listed in figure. The range of rotation is form −10° to 10°. Deformation of CFR joint with moment loading has an approximate symmetry property, and thus Fig. 16 only shows ten γ-values. The set of points from the top down means γ-values corresponding to angle 1°–10°, respectively. Fig. 16 evidently indicates that γ-values fluctuate along with 0.5. It can be easily concluded that γ is approximately equal to 0.5 though the deformation angle increases. Therefore, γ can be 0.5, namely the rotational center is the midpoint of L_1.

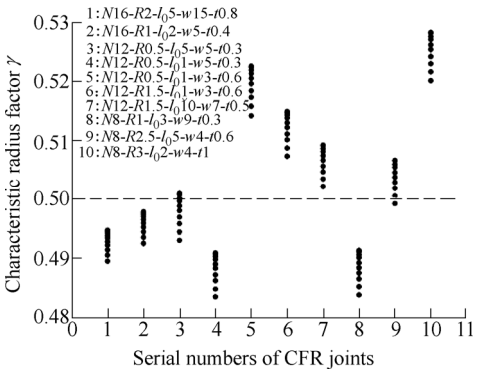

Fig. 16. Characteristic radius factor γ of CFR Joint

6 Conclusions

(1) The new flexure beam designs allow for a larger range of motion than those of conventional flexible structures.

(2) All the stiffness components of CF beam have approximate equations except K_{rx}. These equations have high accuracy and wide applicability.

(3) As both R and l decrease to zero, that is to say, CF beam changes to straight beam, stiffness and the ratio of off-axis to axial stiffness increase to their maximum values. That means stiffness and the ratio have wide ranges and they can be flexibly determined to meet the design requirements.

(4) The empirical equations suffer from some limitations which should be emphasized. There is no explicit equation for K_{rx}, so FEA must be carried out when K_{rx} is needed. When CF beam is loaded in the negative direction of x-axis, there is an axis drift, which will complicate the analysis.

References

[1] KOTA S, HETRICK J, LI Z, et al. Tailoring unconventional actuators using compliant transmissions: design methods and applications[J]. *IEEE/ASME Transactions on Mechatronics*, 1999, 4(4): 396–408.

[2] HOWELL L L. *Compliant mechanisms*[M]. New York: John Wiley & Sons, 2001.

[3] CHANG S H, TSENG C K, CHIEN H C. An ultra-precision $XY\theta_z$ piezo-micropositioner. I. Design and analysis[J]. *Ferroelectrics and Frequency Control, IEEE Transactions on Ultrasonics*, 1999, 46(4): 897–905.

[4] CULPEPPER M L, ANDERSON G. Design of a low-cost nano-manipulator which utilizes a monolithic, spatial compliant mechanism[J]. *Precision Engineering*, 2004, 28(4): 469–482.

[5] FRECKER M I, HALUCK R, POWELL K M. Design of a multifunctional compliant instrument for minimally invasive surgery[J]. *Journal of Biomechanical Engineering*, 2005, 127(6): 990–993.

[6] SEIBOLD U, K BLER B, HIRZINGER G. Prototype of instrument for minimally invasive surgery with 6-axis force sensing capability[C]//*Proceedings of the ICRA*, Barcelona, Spain, April 18–22, 2005: 498–503.

[7] CRONIN J A, MATHEW A, FRECKER M I. Design of a compliant endoscopic suturing instrument[J]. *Journal of Medical Devices*, 2008, 2(2): 025002.

[8] KOTA S. Design of compliant mechanisms: applications to MEMS[C]//*Proceedings of the 1999 Symposium on Smart Structurs and Materials*, San Diego, USA, March 1–5, 1999: 45–54.

[9] SARDAN O, EICHHORN V, PETERSEN D, et al. Rapid prototyping of nanotube-based devices using topology- optimized microgrippers[J]. *Nanotechnology*, 2008, 19(49): 495–503.

[10] ATEN Q T, JENSEN B D, HOWELL L L. Geometrically non-linear analysis of thin-film compliant MEMS via shell and solid elements[J]. *Finite Elements in Analysis and Design*, 2012, 49(1): 70–77.

[11] HOWELL L L, MIDHA A. A method for the design of compliant mechanisms with small-length flexural pivots[J]. *Journal of Mechanical Design*, 1994, 116(1): 280–290.

[12] ANANTHASURESH G K. *A new design paradigm for micro-electro-mechanical systems & investigations on the compliant mechanism sythesis*[M]. Ann Arbor: University of Michigan, 1994.

[13] FRECKER M, ANANTHASURESH G, NISHIWAKI S, et al. Topological synthesis of compliant mechanisms using multi-criteria optimization[J]. *Journal of Mechanical Design*, 1997, 119(2): 238–245.

[14] WANG M Y, WANG X, MEI Y, et al. Design of multimaterial compliant mechanisms using level-set methods[J]. *Journal of Mechanical Design*, 2005, 127(5): 941–956.

[15] WANG N, TAI K. Design of grip-and-move manipulators using symmetric path generating compliant mechanisms[J]. *Journal of Mechanical Design*, 2008, 130(11): 112305.

[16] WANG N, TAI K. Design of 2-DOF compliant mechanisms to form grip-and-move manipulators for 2D workspace[J]. *Journal of Mechanical Design*, 2010, 132(3): 031007.

[17] HAGISHITA T, OHSAKI M. Topology optimization of trusses by growing ground structure method[J]. *Structural and Multidisciplinary Optimization*, 2009, 37(4): 377–393.

[18] SIGMUND O, MAUTE K. Topology optimization approaches[J]. *Structural and Multidisciplinary Optimization*, 2013, 48(6): 1031–1055.

[19] ZHU B, ZHANG X, WANG N. Topology optimization of hinge-free compliant mechanisms with multiple outputs using level set method[J]. *Structural and Multidisciplinary Optimization*, 2013, 47(5): 659–672.

[20] LOBONTIU N. *Compliant mechanisms: design of flexure hinges*[M]. Boca Raton: CRC press, 2002.

[21] SHUIB S, RIDZWAN M, KADARMAN A H. Methodology of Compliant Mechanisms and its Current Developments in Applications: A Review[J]. *American Journal of Applied Sciences*, 2007, 4(3): 160–167.
[22] MOON Y-M, KOTA S. Design of compliant parallel kinematic machines[C]//*Proceedings of the ASME 2002 International Design Engineering Technical Conferences and Computers and Information in Engineering Conference*, Montreal, Canada, September 29–October 2, 2002: 35–41.
[23] PAVLOVIĆ N T, PAVLOVIĆ N D. Compliant mechanism design for realizing of axial link translation[J]. *Mechanism and Machine Theory*, 2009, 44(5): 1082–1091.
[24] KYUSOJIN A, SAGAWA D. Development of linear and rotary movement mechanism by using flexible strips[J]. *Bulletin of the Japan Society of Precision Engineering*, 1988, 22(4): 309–314.
[25] HARINGX J. The cross-spring pivot as a constructional element[J]. *Applied Scientific Research*, 1949, 1(1): 313–332.
[26] SMITH S T. *Flexures: elements of elastic mechanisms*[M]. Boca Raton: CRC Press, 2000.
[27] MOON Y-M, TREASE B P, KOTA S. Design of large-displacement compliant joints[C]//*Proceedings of the ASME 2002 International Design Engineering Technical Conferences and Computers and Information in Engineering Conference*, Montreal, Canada, September 29–October 2, 2002: 65–76.
[28] FETTIG H, WYLDE J, HUBBARD T, et al. Simulation, dynamic testing and design of micromachined flexible joints[J]. *Journal of Micromechanics and Microengineering*, 2001, 11(3): 209.
[29] WANG N, LIANG X, ZHANG X. Pseudo-rigid-body model for corrugated cantilever beam used in compliant mechanisms[J]. *Chinese Journal of Mechanical Engineering*, 2014, 27(1): 122–129.
[30] OHWOVORIOLE M, ROTH B. An extension of screw theory[J]. *Journal of Mechanical Design*, 1981, 103(4): 725–735.
[31] SU H-J, DOROZHKIN D V, VANCE J M. A screw theory approach for the conceptual design of flexible joints for compliant mechanisms [J]. *Journal of Mechanisms and Robotics*, 2009, 1(4): 041009.
[32] HOPKINS J B, PANAS R M. Design of flexure-based precision transmission mechanisms using screw theory[J]. *Precision Engineering*, 2013, 37(2): 299–307.
[33] CHENG D. *Mechanical design handbook*[M]. Beijing: Chemistry Industry Publisher, 2004.
[34] WANG J, CHEN J-K, LIAO S. An explicit solution of the large deformation of a cantilever beam under point load at the free tip[J]. *Journal of Computational and Applied Mathematics*, 2008, 212(2): 320–330.
[35] JONES R M. *Mechanics of composite materials*[M]. Boca Raton: CRC Press, 1998.

Biographical notes

WANG Nianfeng, born in 1977, is currently a professor at *South China University of Technology, China.* He received his PhD degree from *Nanyang Technological University, Singapore*, in 2008. His research interests include compliant mechanism, structural optimization and robotics.
Tel: +86-20-87110059; E-mail: menfwang@scut.edu.cn

LIANG Xiaohe, born in 1989, is currently a master candidate at *South China University of Technology, China*. His research interests include compliant mechanism, precision equipment.
E-mail: 746155882@qq.com

ZHANG Xianmin, born in 1964, is currently a professor at *South China University of Technology, China.* He received his PhD degree from *Beihang University, China*, in 1997. His research interests include mechatronics engineering, compliant mechanism.
Tel: +86-20-87110059; E-mail: zhangxm@scut.edu